(4) Nagarajan, R. *Polym. Prepr., Am. Chem. Soc. Div. Polym. Chem.* **1981**, *22*, 33.
(5) (a) Dong, D. C.; Winnik, M. A. *Photochem. Photobiol.* **1982**, *35*, 17. (b) Nakajima, A. *J. Lumin.* **1976**, *11*, 429 and early papers.
(6) Kalyanasundaram, K.; Thomas, J. K. *J. Am. Chem. Soc.* **1977**, *99*, 2039.
(7) (a) Turro, N. J.; Tanimoto, Y.; Gabor, G. *Photochem. Photobiol.* **1980**, *31*, 527. (b) Schore, N. E.; Turro, N. J. *J. Am. Chem. Soc.* **1975**, *97*, 2488.
(8) Arai, H.; Murata, M.; Shinoda, K. *J. Colloid Interface Sci.* **1971**, *37*, 223.
(9) Shirakama, K. *Colloid Polym. Sci.* **1974**, *252*, 978.
(10) Zana, R. *Polym. Prepr., Am. Chem. Soc., Div. Polym. Chem.* **1982**, *23*, 41.
(11) Takagishi, T.; Kuroki, N. *J. Polym. Sci., Polym. Chem. Ed.* **1973**, *11*, 1889.
(12) Arkhipovich, G. N.; Dubronski, S. A.; Kazanski, K. S.; Ptitsina, K. S.; Shupik, A. N. *Eur. Polym. J.* **1982**, *18*, 569.

On the Nature of the Poly(γ-benzyl glutamate)–Dimethylformamide "Complex Phase"

Paul S. Russo† and Wilmer G. Miller*

Department of Chemistry, University of Minnesota, Minneapolis, Minnesota 55455.
Received May 17, 1983

ABSTRACT: The system poly(γ-benzyl L-glutamate)/dimethylformamide (PBLG/DMF) has been studied by small-angle X-ray scattering, polarizing optical microscopy, differential scanning calorimetry, and visual observation. The effects of a nonsolvent, water, have been assessed. We find that a small amount of water, which can be easily absorbed from the atmosphere under normal ambient conditions, even when samples are stored in capped containers, seriously alters the visual appearance, phase behavior, and morphology of the system. The various morphologies available in PBLG/DMF/H_2O are classified and discussed in terms of a pseudobinary, biphasic system, in which a polymer-rich ordered state coexists with a polymer-poor phase, which may be ordered or disordered depending on water content and temperature. We conclude that the "complex phase" reported for PBLG/DMF is a result of water contamination and is related to the phase behavior of the PBLG/DMF/H_2O ternary system.

Introduction

Poly(γ-benzyl L-glutamate) (PBLG) was the first synthetic polymer to exhibit cholesteric liquid crystalline behavior in solution.[1,2] A cholesteric phase is known to exist in a number of solvents.[4–10] However, there is disagreement over the morphological state in dimethylformamide (DMF). In two independent X-ray investigations on the PBLG/DMF system, a "complex phase" was reported.[11,12] This state, which occurred below ca. 40 °C, was described as an opaque gel.[11] Watanabe et al. noted an opaque gel at $T < 60$ °C in 20 wt % PBLG/DMF.[8] Over the years, opaque whitish states have occasionally been seen in this laboratory. However, the vast majority of PBLG/DMF samples have been clear, with the cholesteric thumbprint pattern clearly evident in the polarizing optical microscope.[1–3] Many flame-sealed samples,[13,14] used to determine the phase boundaries in this system, have remained clear for a decade. The occasional whitish samples have been routinely discarded in the belief that a nonsolvent, such as water, caused the whitish appearance.

In this paper, we report the findings of a reexamination of both clear and whitish samples. Using small-angle X-ray scattering (SAXS), polarizing optical microscopy (POM), differential scanning calorimetry (DSC), and visual observations, we have determined the effect of a small amount of water. For comparison, the effect of a nonsolvent on the phase behavior has also been calculated. We conclude that a small amount of water drastically changes the appearance and morphology of the system in a fashion consistent with its phase behavior.

Materials and Methods

PBLG of 310 000 and 130 000 daltons (M_w) was obtained from New England Nuclear and Miles Yeda, respectively, and designated as PBLG-310000 and PBLG-130000. On the basis of the polymerization mechanism and results from other studies,[15a] M_w/M_n is considered to be 1.2–1.3. PBLG was vacuum-dried to constant weight at temperatures not exceeding 60 °C prior to use. Reagent grade DMF was dried over 4-Å molecular sieves and distilled under reduced pressure at ca. 50 °C. Solutions were prepared by weight in a dry atmosphere or as rapidly as possible in the open atmosphere. Solutions were homogenized in capped vials containing magnetic stirbars placed on a stirring hotplate in a dry nitrogen atmosphere. The temperature required for dissolution increased with water content. If necessary, the temperature was raised to as much as 80–100 °C for a short time to ensure homogeneous samples. For conversion to volume fraction (v_p), the specific volume of PBLG was taken as 0.791 cm^3/g and the density of DMF as 0.944 g/cm^3.

All X-ray studies were performed in 1-mm glass capillaries with 0.01-mm-thick walls (Charles Supper Co.). The sample was transferred into the capillary and spun to the bottom in a low-speed centrifuge, both operations taking place under a dry nitrogen atmosphere. The capillaries were removed from the dry atmosphere and immediately flame sealed. A good seal was ensured by dunking the capillary tip several times into molten beeswax. The capillaries were then weighed over a period of several days to check for leaks. The delicate capillaries were stored inside tubular holders glued to microscope slides held in a slide box. Temperature equilibration was achieved by immersing a watertight slide box into a temperature-controlled bath (±0.005 °C). The samples were transported to the X-ray camera in a capped Dewar containing some water from the bath. The sample was mounted in a brass cell holder of original design. The holder had a volume of 3 $in.^3$, through which thermostated water circulated, and was designed to fit into the standard slots of the Warhus pinhole-collimated camera used throughout these studies. Kel-F insulators prevented heat transfer to the rest of the camera, and the water inlet lines were sealed to permit vacuum operation for reduced air scatter. Since facilities for measurement of the temperature at the brass block during the measurement were not available, the temperature reported is that at the water bath, which was connected to the cell holder by well-insulated lines. All measurements were performed under vacuum. The camera had several standard film positions. The distance from the sample

†Present address: Department of Chemistry, Louisiana State University, Baton Rouge, LA 70803.

0024-9297/84/2217-1324$01.50/0

to the closest of these was calibrated by measuring the diffraction from a finely ground sample of ACS grade sodium chloride, which loosely adhered to a capillary that had been dunked into a toluene slurry and allowed to dry. Adding the known distance between the film plane actually used and that which was calibrated gave a working distance of 16.93 cm. The X-ray source was a Siemens FK60-20 Cu tube, primarily designed for slit-collimated output. Consequently, most of the available X-rays were absorbed by the input pinholes, and long exposures, typically 10 h at 40 kV and 40 mA, were required.

Visual observations were made from the X-ray capillaries or from sealed cells with either 1-mm or 1.5-mm path length. A Leitz polarizing optical microscope was used for microscopic observation. Visual clearing points were determined for whitish samples in sealed melting point capillaries, using a standard Fisher melting point apparatus. A drop of oil ensured good thermal contact. Sharp "melting" transitions (1–2 °C), defined as the temperature at which the sample clarified, were observed at heating rates of ca. 1 °C/min.

DSC measurements were taken on a Perkin-Elmer DSC-2 with liquid nitrogen as coolant. The instrument was calibrated with water and DMF, and temperatures were accurate to ±1 °C. Samples of PBLG-310000 were made at 18 vol % (24 wt %) in 0–5.0 vol % aqueous DMF and homogenized as described above. Six to ten milligrams of sample was placed onto weighed aluminum sample pans in the open atmosphere, and the pans were then quickly sealed by crimping. Pans were checked by weight for leakage of solvent; defective samples were discarded. Thermograms, usually at 10 °C/min, were run in the range 150–350 K.

Results

Visual and Microscopic Observations. It has proved convenient to classify PBLG/DMF/H_2O samples according to visual and microscopic appearance. The scheme presented applies to samples of 1-mm thickness.

Clear Samples. Clear Cholesteric: The sample is visually clear and has the characteristic cholesteric "thumbprint" pattern of periodicity lines evident in the POM.[1-3] The clear cholesteric state is found in samples with polymer volume fraction $v_p \leq 0.30$ in dry DMF at temperatures as low as 15 °C; it is also found in samples with $v_p < 0.30$ in wet DMF, but only above about 35 °C. This state is fluid.

Rainbow Cholesteric: The sample is not opaque; however, images viewed through it are distorted. Myriad colors are seen even in natural light; the cholesteric thumbprint pattern is observed in the POM. This state is found in samples with $v_p > 0.30$. These samples may turn pearly (in dry DMF) or whitish (in wet DMF) upon aging, with no periodicity lines observable. The rainbow cholesteric state is fluid.

Pearly: The sample has a white hue but is not opaque. This state is common to aged (at room temperature), concentrated ($v_p > 0.30$) samples in dry DMF. It appears to be a very viscous fluid. More dilute samples in dry DMF at subambient temperatures have the same appearance.

Opaque Samples. Cloudy: This is a turbid state, intermediate between the clear cholesteric state and the whitish state. This is sometimes seen in dilute ($v_p < 0.30$) *unaged* samples in wet DMF. The sample is fluid, but slurry-like.

Whitish: The sample is white and thoroughly opaque. No POM observations can be made. This state occurs in *aged*, water-contaminated samples or in new samples with severe water contamination. The state is not fluid. At temperatures exceeding 35 °C, whitish samples almost invariably melt into clear or rainbow cholesteric states, periodicity lines are immediately evident in the POM, and the sample flows.

Whenever great caution is taken to dry the DMF and *keep* the sample dry, whitish or cloudy states are not seen. The visual appearance of the samples prepared for DSC and visual clearing points was followed over a period of

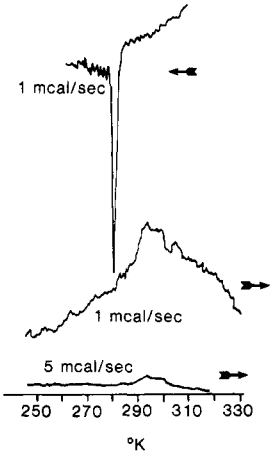

Figure 1. DSC thermograms for an 18 vol % (24 wt %) PBLG-310000/DMF sample containing 1 vol % H_2O. Sensitivity and direction of scanning are indicated.

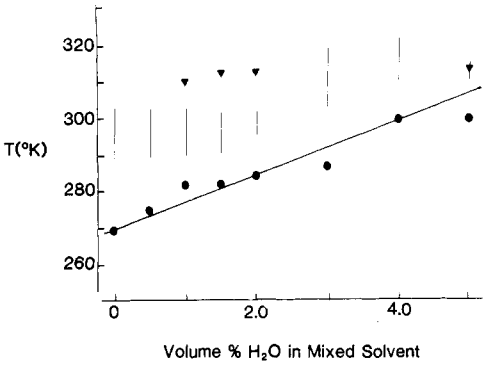

Figure 2. DSC exothermic peak on cooling (●), onset of endothermic peak on heating (|), and visual clearing temperature (▼) as a function of water content for the system PBLG-310000/DMF/H_2O.

3 months. Solutions with $v_p = 0.18$ (PBLG-310000) and varying water content were stored in tightly capped machine vials at room temperature in a desiccator filled with a dry, DMF-saturated atmosphere. Samples with water content exceeding 0.5 vol % turned whitish over a period of hours to weeks, depending on the water content. Only the samples prepared in dry DMF and at 0.5 vol % water remained clear. Many samples of the dry cholesteric phase at various compositions when left in the laboratory atmosphere in "tightly capped" vials turn whitish over a period of months. However, dry samples sealed in glass tubes since 1969 have remained clear. Thus the appearance of whitish PBLG/DMF samples is an indication of water contamination. The whitish state is generally a gel, as is the clear state below ca. 10 °C.[15b]

DSC and Visual Melting Points. On heating, a DSC endotherm was observed, associated with the enthalpy of the wide biphasic to single-phase cholesteric transition.[17] This broad endotherm was found to depend on the water content of the sample. In some aged, wet samples, a fine structure, including two peaks, was seen. On cooling, supercooling was noted, followed by a sharp exotherm lying some 20–30 °C below the broad melting endotherm. If the molten sample was quenched at 160 °C/min, the endotherm upon reheating was diminished and distorted. If the sample was then cooled slowly at 10 °C/min, the sharp exotherm was seen. Upon heating, the broad endotherm reappeared. Some of these observations are shown in Figure 1. The temperature of both the endotherms on heating and the exotherms on cooling increased with water content (Figure 2). The sharpness of the exotherms gives a more reliable estimate of the shift in transition tem-

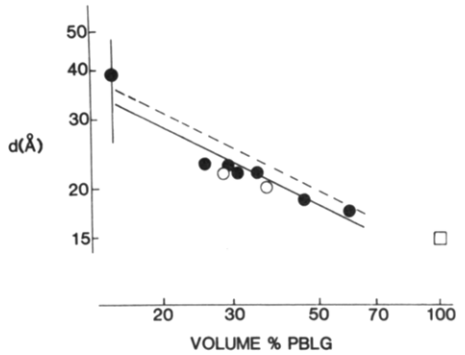

Figure 3. X-ray spacings in PBLG/DMF as a function of concentration at 40 °C compared to that expected of hexagonal (—) or cubic (– – –) packing of rods. Open circles, samples were opaque and white at room temperature; filled circles, samples were clear at room temperature (see text). The spacing in a film prepared by evaporation of DMF from a dilute solution is also shown (□).

perature. The addition of only 4 vol % water shifts the transition temperature ca. 30 °C.

The visual change of wet, whitish samples into a clear state was much sharper than the corresponding DSC endotherm; typically, the whitish-to-clear transition occurred over only ±1 °C (Figure 2). The pearly-to-clear transition for solutions with less than 1% water is hard to follow visually and is therefore not reported. The visual transition occurred at a higher temperature than the DSC transition. Heat transfer in the melting point apparatus is much slower than in the DSC sample pan; however, the heating rate in the DSC was larger. Some of the difference between the two types of transition temperature may be due to these factors.

At low temperatures, below ca. −10 °C, where one is well within the isotropic–liquid crystalline wide biphasic region, the room-temperature "clear cholesteric" samples do not exhibit periodicity lines by POM. Upon warming to the single-phase liquid crystal region, hours to days may be required before periodicity lines are observable, depending on sample composition. However, whitish samples, when heated from low temperature to the clearing temperature or above, immediately show periodicity lines. The initial periodicity spacings after warming are typically smaller than the long-time values.

X-ray Observations. The concentration dependence of the intermolecular spacing in cholesteric samples of PBLG-130000/DMF at 40 °C is shown in Figure 3. The slope of this log–log plot is about −0.5, suggesting a two-dimensional array. The deviation from strict −0.5 dependence is similar to that observed by Robinson.[2] Since higher order peaks were not seen, the circumspect indexing method of Robinson was applied. The spacings expected for two-dimensional cubic and hexagonal packing are shown. The data clearly lie closer to the line for hexagonal packing, as was the case in dioxane.[2]

In optically clear samples, long-range liquid crystalline order may be seen in the POM at concentrations as low as 15 wt %. However, below ca. 25 wt % it becomes impossible to detect an X-ray spacing, even with very long exposures (24 h). On the other hand, whitish samples at 25 °C gave multiple, sharp X-ray spacings even for polymer concentrations as low as 16 wt %. Unlike the cholesteric samples, whitish and pearly samples below ca. 35 °C gave spacings that were concentration invariant. The spacings for pearly or whitish samples (Table I) nearly match the strong spacings seen by Parry and Elliot[12] and Luzzati et al.,[11] who also noted the concentration invariance. We did on occasion (Table II) also detect the weaker spacings reported by Parry and Elliott and Luzzati et al.

Table I
X-ray Spacings in Whitish or Pearly Samples

spacing, Å	intens	breadth	hexagonal spacing
32	very strong	±3 Å (typical)	d_{100} (system A)
18.5 ± 0.5	moderate	sharp	d_{110} (system A)
15.5 ± 0.5	moderate	sharp	d_{200} (system A); d_{100} (system B)

Table II
Additional X-ray Spacings Observed Occasionally in Whitish or Pearly Samples

spacing, Å	intens	comment
11.6 ● 0.3	weak	d_{210} (system A)
10.2	weak	stacking interaction[12]
9.0	weak	d_{110} (system B)
5.1	weak	stacking interaction[12]

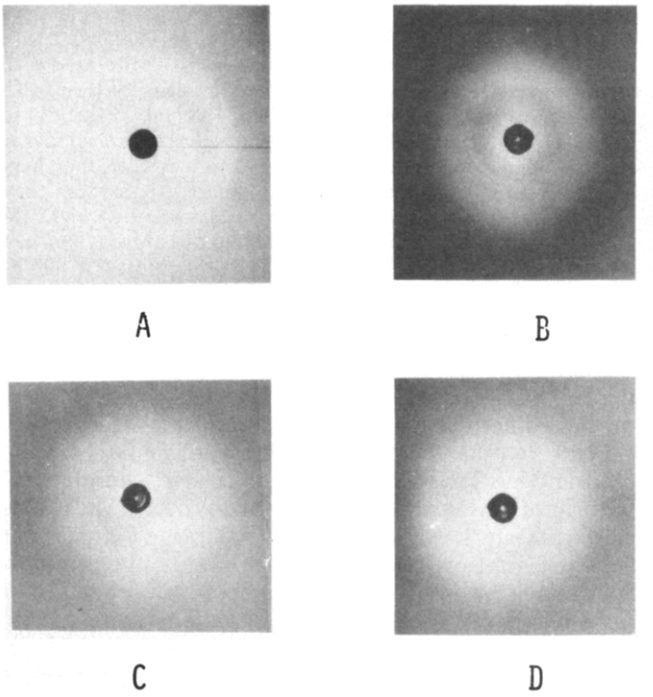

Figure 4. X-ray pattern of a whitish (room temperature) 29 vol % (35 wt %) PBLG-130000/DMF sample at 25 (A), 30 (B), 35 (C), or 40 °C (D).

Since we have noted that a whitish sample melts instantaneously into the cholesteric state and since we have followed this calorimetrically and visually, it was thought that X-ray studies might reveal more about the structural evolution as a function of temperature. A whitish 28.5 vol % (34.8 wt %) sample had the spacings listed in Table I at room temperature (see Figure 4A). At 40 °C, the sample, now clear, had a single diffuse spacing at 21.8 Å (Figure 4D). At intermediate temperature (Figure 4B,C) diffraction peaks characteristic of both whitish and cholesteric samples were evident. As the temperature was raised, the whitish spacings gradually weakened. The pattern in Figure 4C was taken after 4 days of equilibration at 35 °C. Some evidence of the whitish spacing remained as a greatly weakened, but still sharp, 32.6 Å spacing. These measurements were done nonsequentially regarding temperature with at least a 20-h equilibration period. This suggests equilibrium coexistence of the structures leading to whitish and cholesteric states at this temperature.

In Figure 5A–D, a 60 vol % (67 wt %) PBLG-130000 sample, prepared scrupulously dry before capillary loading, displayed similar but somewhat simpler behavior on transition from pearly to rainbow cholesteric. At room temperature, the X-ray pattern showed all the spacings

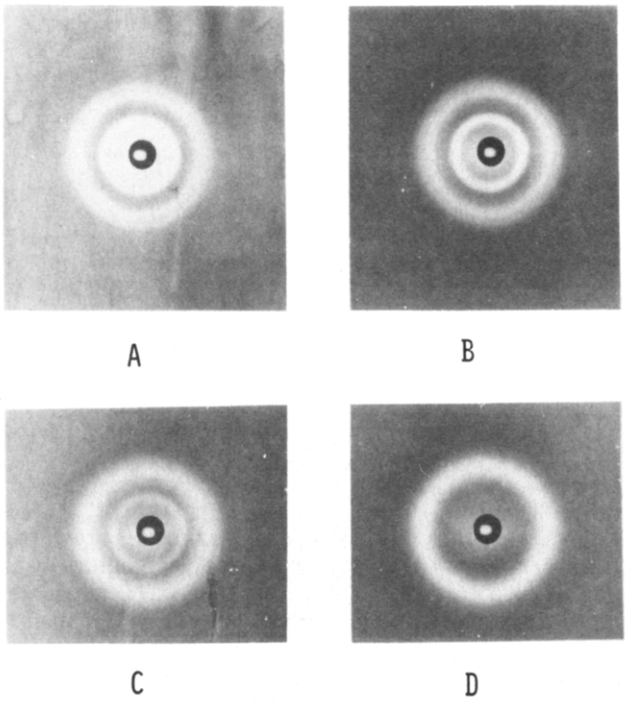

Figure 5. X-ray pattern of a 60 vol % (67 wt %) PBLG-130000 sample at 25 (A), 33 (B), 38 (C), or 44 °C (D).

of Table I and some of those of Table II. The pattern is consistent with the simultaneous presence of two hexagonal lattices. Lattice A has $d_{100}^{A} = 32.9 \pm 4.3$ Å with $d_{110}^{A} = 18.3$ Å and $d_{200}^{A} = 15.6$ Å. Lattice B has $d_{100}^{B} = 15.6$ Å and $d_{110}^{B} = 9.0$ Å. At 33 °C, the d_{210}^{A} spacing, 11.7 Å, has appeared. By 38 °C, the d_{110}^{B} spacing is no longer evident. There is also considerable weakening of the heavy spacing, now at 31.8 ± 3 Å, and it is difficult to distinguish the d_{110} and d_{200} peaks, as they overlap with the emergent cholesteric diffuse peak, 17.4 Å, which dominates at 44 °C. Like Figure 4A–D, this series was measured in nonsequential order, but with equilibration times of as little as 5 h. This series is again consistent with the coexistence of two ordered phases in the intermediate temperature zone. It suggests that the structure in at least one of the phases might be fairly detailed.

The solvent content of each of the X-ray samples must be approached with care. Water vapor generated during flame sealing sometimes entered the loaded capillaries, as evidenced by a sealed sample turning whitish at room temperature upon standing. X-ray observations on phase behavior in supposedly dry samples may, in fact, be on samples with some water contamination. Thus the measurements on the 60 vol % sample could be on a sample with some water contamination.

Discussion

There can be little doubt that water contamination of DMF profoundly affects the morphology seen at a given temperature. This fact almost certainly lies at the core of the controversy as to the goodness of DMF as a solvent for PBLG. Goebel and Miller[18] have reported positive virial coefficients for PBLG in DMF above ca. 22 °C, approaching the excluded volume value at about 40 °C. On the other hand, Watanabe et al. list DMF as a poor solvent by qualitative judgment.[8] Likewise, while some workers[13,14] have reported clear cholesteric solutions at room temperature, others have obtained whitish samples.[11] From visual and DSC melting points we have found that water strongly modifies the thermal behavior of the system. From a thermodynamic point of view, this may result from

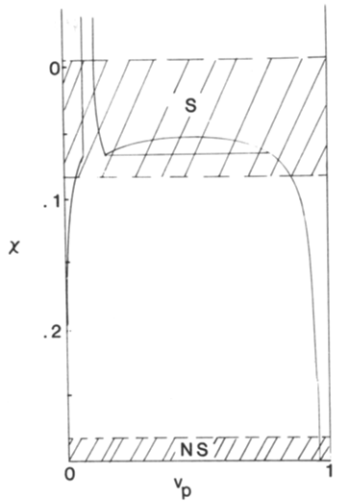

Figure 6. Phase behavior of rigid rod polymer–diluent by the Flory theory for axial ratio 100. Phases are isotropic (I) or liquid crystalline (LC). See text for meaning of S and NS.

an increase in the solvent–polymer interaction free energy. For liquid crystalline solutions of rigid rods, phase separation is predicted to occur at only slightly positive χ values, depending on axial ratio and concentration.[19] The transition observed[14,20] in dry DMF occurs at 15–20 °C at concentrations below 30 vol % PBLG. One would expect water, a known nonsolvent, to raise the transition temperature. The results certainly confirm this expectation.

It is felt that failure to fully appreciate the hygroscopicity of DMF has led to the disagreements over the PBLG/DMF system. Even under "dry" atmospheric conditions of 25% relative humidity, DMF can take up to 14% water.[20] Karl Fischer titrations performed in this laboratory have amply demonstrated the hygroscopic nature of DMF when exposed to normal room conditions. Although the solvent is not difficult to dry, one cannot overemphasize the importance of keeping the sample dry by storing over a desiccant, or when flame sealing, being careful that water vapor from the flame does not contaminate the sample.

The results on the effect of water can best be understood through its effect on polymer–diluent phase equilibria. All features of the binary polymer–diluent phase behavior of rigid rod polymers predicted by the Flory model[19,21] (Figure 6) have been observed for the PBLG/DMF system,[13,14,16,20] including the existence of the liquid crystal–liquid crystal (LC–LC) biphasic region.[20] Two polymer–solvent–nonsolvent ternary systems have been investigated.[13,22] Cloud point curves for the PBLG/DMF/H_2O system suggest that a biphasic region can be entered at 30 °C with as little as 1 vol % water.

Ternary diagrams based on the binary polymer–solvent (P–S) Flory model[19] can be calculated after generalization to include a second solvent (NS). The chemical potentials in the isotropic phase, μ_i^{I}, relative to those of the pure components, $\mu_i°$, become

$$(\mu_S^{I} - \mu_S°)/RT = \ln v_S + (1 - 1/x)v_P + (\chi_{S\text{-}NS}v_{NS} + \chi_{S\text{-}P}v_P)(v_{NS} + v_P) - \chi_{NS\text{-}P}v_{NS}v_P \quad (1)$$

and

$$(\mu_{NS}^{I} - \mu_{NS}°)/RT = \ln v_{NS} + (1 - 1/x)v_P + (\chi_{S\text{-}NS}v_S + \chi_{NS\text{-}P}v_P)(v_S + v_P) - \chi_{S\text{-}P}v_Sv_P \quad (2)$$

and

$$(\mu_P^{I} - \mu_P°)/RT = \ln (v_P/x) + (x - 1)v_P - 2 \ln x + (\chi_{S\text{-}P}v_S + \chi_{NS\text{-}P}v_{NS})(v_S + v_{NS})x - x\chi_{S\text{-}NS}v_Sv_{NS} \quad (3)$$

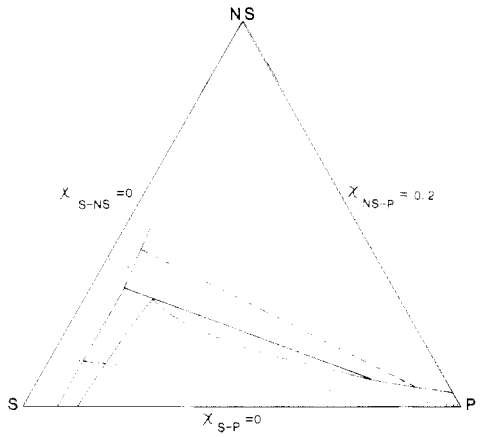

Figure 7. Ternary phase diagram for a rigid rod polymer (P) of axial ratio 100 in the presence of two diluents (S and NS) for the binary interaction parameters χ_{i-j} as shown. Phases present in each region can be identified by analogy to Figure 6. The phase boundaries are given by solid lines, tie lines by dashed lines, and lines of constant S/NS ratio by dotted lines.

where x is the polymer axial ratio and χ_{i-j} are the binary interaction parameters. In the liquid crystalline phase, the chemical potentials, μ_i^{LC}, become, when $y > 1$,

$$(\mu_S^{LC} - \mu_S^\circ)/RT = \ln \upsilon_{NS} + (y-1)\upsilon_P/x + 2/y + (\chi_{S-NS}\upsilon_{NS} + \chi_{S-P}\upsilon_P)(\upsilon_{NS} + \upsilon_P) - \chi_{NS-P}\upsilon_{NS}\upsilon_P \quad (4)$$

and

$$(\mu_{NS}^{LC} - \mu_{NS}^\circ)/RT = \ln \upsilon_{NS} + (y-1)\upsilon_P/x + 2/y + (\chi_{S-NS}\upsilon_S + \chi_{NS-P}\upsilon_P)(\upsilon_S + \upsilon_P) - \chi_{S-P}\upsilon_S\upsilon_P \quad (5)$$

and

$$(\mu_P^{LC} - \mu_P^\circ)/RT = \ln (\upsilon_P/x) + (y-1)\upsilon_P + 2 - 2\ln y + (\chi_{S-P}\upsilon_S + \chi_{NS-P}\upsilon_{NS})(\upsilon_S + \upsilon_{NS})x - x\chi_{S-NS}\upsilon_S\upsilon_{NS} \quad (6)$$

under the constraint

$$\upsilon_P = [x/y(x-y)][1 - \exp(-2/y)] \quad (7)$$

where y is the disorientation parameter. At concentrations where the disorientation parameter is unity, eq 4–6 are replaced by

$$(\mu_S^{LC} - \mu_S^\circ)/RT = \ln \{\upsilon_S/[1 - (1 - 1/x)\upsilon_P]\} + (\chi_{S-NS}\upsilon_{NS} + \chi_{SP}\upsilon_P)(\upsilon_{NS} + \upsilon_P) - \chi_{NS-P}\upsilon_{NS}\upsilon_P \quad (8)$$

and

$$(\mu_{NS}^{LC} - \mu_{NS}^\circ)/RT = \ln \{\upsilon_{NS}/[1 - (1 - 1/x)\upsilon_P]\} + (\chi_{S-NS}\upsilon_S + \chi_{NS-P}\upsilon_P)(\upsilon_S + \upsilon_P) - \chi_{S-P}\upsilon_S\upsilon_P \quad (9)$$

and

$$(\mu_P^{LC} - \mu_P^\circ)/RT = \ln \{(\upsilon_P/x)/[1 - (1 - 1/x)\upsilon_P]\} + (\chi_{S-P}\upsilon_S + \chi_{NS-P}\upsilon_{NS})(\upsilon_S + \upsilon_{NS})x - x\chi_{S-NS}\upsilon_S\upsilon_P \quad (10)$$

Phase equilibria may be calculated from the chemical potentials. A ternary diagram with $\chi_{S-NS} = \chi_{S-P} = 0$ and $\chi_{NS-P} = 0.2$ is shown in Figure 7. The similarity between the binary and ternary diagrams is evident. Three features are worthy of note: (1) in the narrow biphasic region the tie line and the line of constant nonsolvent/solvent ratio are nearly coincident, whereas in the wide I–LC biphasic or the LC–LC region they generally are not coincident; (2) in order for 1% water (NS component) to force the system into the LC–LC region at some polymer compositions, as suggested by previous data,[22] χ_{NS-P} and χ_{S-P} must be more positive than the values used in calculating Figure 7, as, for example, shown in Figure 8; (3) if samples are diluted along certain lines of fixed nonsolvent/solvent ratio, the phases in equilibrium can change from I–LC (wide biphasic) to LC–LC. The implications of the first feature are significant. It suggests that in the narrow biphasic region a solvent/nonsolvent pair may be considered a proper pseudocomponent and the phase diagram reduced to a pseudobinary, whereas this would not generally be true in other regions of the phase diagram. The underlying basis for this can be determined. For I–LC as well as LC–LC equilibria it can be shown that

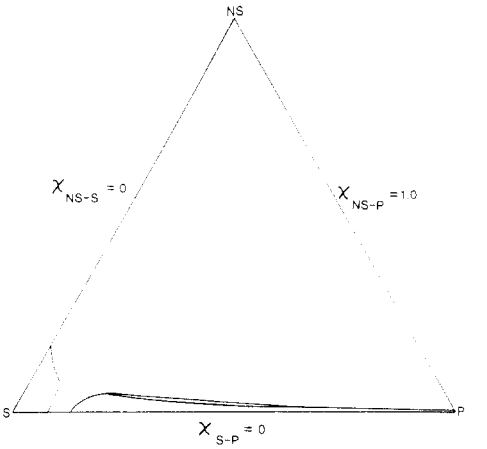

Figure 8. Effect of increasing the polymer–nonsolvent incompatibility (χ_{P-NS}) over that in Figure 7.

$$(\upsilon_S''/\upsilon_{NS}'')/(\upsilon_S'/\upsilon_{NS}') = \exp\{(\chi_{NS-P} - \chi_{S-P}) \times (\upsilon_P'' - \upsilon_P') + \chi_{S-NS}[(\upsilon_{NS}' - \upsilon_S') - (\upsilon_{NS}'' - \upsilon_S'')]\} \quad (11)$$

where double primes indicate the more concentrated polymer phase and single primes the more dilute. So long as the right-hand side is near unity the ternary can be reduced to a pseudobinary. If $\chi_{S-NS} \approx 0$, the pseudobinary approximation depends only on the difference between two χ values, χ_{NS-P} and χ_{S-P}, and the difference in polymer composition between the two phases. In the narrow biphasic region $\upsilon_P'' - \upsilon_P'$ is typically less than 0.05 and sometimes as low as 0.01; thus the system behaves as a pseudobinary one for even widely differing values of χ_{NS-P} and χ_{S-P}; however, in the I–LC wide biphasic region or in the LC–LC region, where $\upsilon_P'' - \upsilon_P'$ may be several tenths, only a small difference in the χ values may lead to the solvents partitioning differentially between the two phases, in which case treating the system as a pseudobinary could be very inappropriate. Solvent partitioning has previously been inferred from phase behavior.[13] Since we have shown that samples thought to be binary may in fact be ternary due to water contamination unknown to the investigator, it is of interest to calculate pseudobinary diagrams to answer the following questions resulting from our studies on the PBLG/DMF/H_2O system: (1) could the "whitish" sample be biphasic as a result of water contamination; (2) can the concentration-independent X-ray spacings of the whitish samples, e.g., about 32 Å at room temperature, be explained, as well as the temperature dependence; (3) why are the wet samples white at room temperature; (4) can the existence of periodicity spacings immediately upon heating to the clearing point be explained?

The first question can be investigated by calculating pseudobinary diagrams from ternary ones. Parameters were chosen through the following considerations: $\chi_{S-NS} \equiv \chi_{DMF-H_2O}$ was taken as zero at all temperatures on the basis that water and DMF are completely miscible at all compositions and temperatures in the liquid state and that addition of up to a few percent water to DMF lowers the

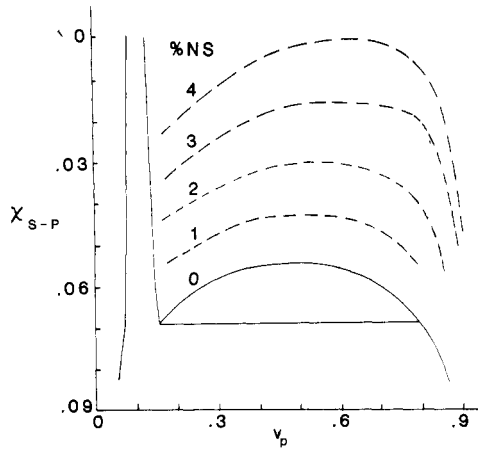

Figure 9. Effect of water contamination on the pseudobinary phase equilibria in the PBLG/DMF/H_2O system. Dashed lines are cloud points determined from the ternary diagram, calculated with $\chi_{S-NS} = 0$, $\chi_{NS-P} = 1.0$, and $x = 100$. The amount of nonsolvent (% NS) was calculated as $100[v_{NS}/(v_S + v_{NS})]$.

DMF freezing point (−61 °C) according to ideal solution behavior for the solution phase; $\chi_{NS-P} \equiv \chi_{H_2O-PBLG}$ was taken as 1 and temperature invariant on the basis that the polymer is not soluble in water to a measurable degree at any temperature; $\chi_{S-P} \equiv \chi_{DMF-PBLG}$ was varied between 0.1 and 0 (see Figure 6), since in dry DMF the LC–LC region appears to lie slightly below room temperature[16,20] and negative χ values are rarely encountered. With these assumptions a series of ternary diagrams was calculated for an axial ratio of 100, with variations in χ_{S-P} corresponding to variation (inversely) in temperature. From these, pseudobinary diagrams were constructed, as shown in Figure 9. A point on a phase boundary can be viewed as the point of phase separation when a fixed composition is cooled or as a cloud point obtained as the point of phase separation when a S/P ratio at fixed temperature (χ) is titrated with the nonsolvent component, NS. Calculations for an axial ratio of 150, more appropriate for 310 000 molecular weight PBLG, shifts the results in a quantitative but not qualitative manner. Because of the solvent/nonsolvent pseudocomponent nature of the system in the narrow biphasic region, only the true binary is shown, which differs little from that for water-contaminated systems. Thus one could not easily detect water contamination by determining the phase boundaries in the narrow biphasic region. However, outside this narrow biphasic region the pseudo-phase boundary is moved steadily to lower χ_{S-P}, i.e., higher temperature, by increasing amounts of water. Addition of 5% water shifts the boundary to negative χ_{S-P}. The cloud point boundaries are insensitive to small variations in χ_{S-NS} and χ_{NS-P}. From these results one can see that the 30 °C shift in calorimetric transition temperature by addition of only 4% water is not unreasonable and gives support to the assertion that the "whitish phase" at various compositions and at temperatures below 40 °C is actually a biphasic sample. Thus there is ample evidence to assert that the "complex phase" deduced from X-ray diffraction[8,11,12] may, in fact, be biphasic.

The second question can also be discussed with respect to Figure 9. In the true two-component system (0% NS) the tie lines are horizontal when the system is in a two-phase region. When water is present and the polymer concentration is varied at fixed temperature, what is the concentration and nature of the phases under the cloud point curves in the pseudobinary diagrams? The answer to this can be obtained from the true ternaries and will be illustrated at two χ_{S-P}'s (temperatures), 0.05 and 0.03.

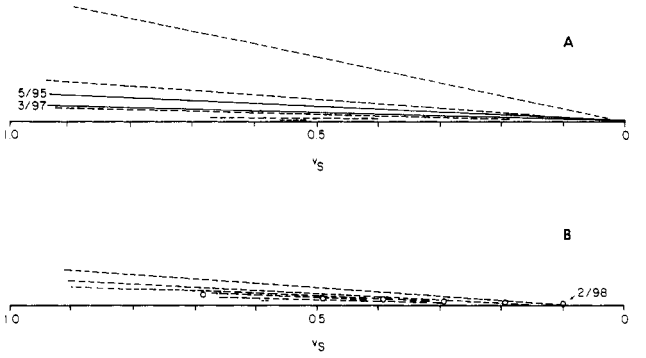

Figure 10. Tie lines (---) and lines (—) or points (O) of constant nonsolvent/solvent ratio with $\chi_{S-P} = 0.05$ (A) or 0.03 (B), taken to correspond to room temperature (A) or higher than 25 °C but less than 40 °C (B). In (A) the bottom two tie lines and in (B) the bottom three tie lines connect LC–LC phases; the remainder connect I–LC phases.

Inasmuch as the LC–LC dome lies slightly below room temperature in the true binary, a χ_{S-P} of 0.05 was taken to represent room temperature, and 0.03 was taken to represent a higher temperature but below 40 °C for the water-wet samples. Appropriate tie lines are shown in Figure 10, along with the dilution lines (Figure 10A) or points along a dilution line (Figure 10B), for fixed nonsolvent (NS)/solvent (S) ratio. For $\chi_{S-P} = 0.05$ (Figure 10A) with a 3/97 nonsolvent to solvent ratio the equilibria for samples of 15–60 vol % polymer are between the *isotropic phase* containing only a few percent polymer and an *ordered phase* of high polymer concentration and only slightly varying composition. For a 5/95 ratio the results are similar. At very low water content a single ordered phase would be encountered. At somewhat higher water contamination, but below 3% nonsolvent, with some sample compositions *two ordered phases* would be in equilibrium at the lower polymer concentrations, but at higher concentrations, a *dilute isotropic* phase would be in equilibrium with the *high-concentration ordered phase*. It seems likely that only the high-concentration ordered phase would be seen by X-ray diffraction, and its composition would not depend significantly on the amount of water contamination or the polymer concentration. Thus one can understand how arbitrary water contamination could give a room-temperature diffraction pattern that was independent of polymer concentration, the pattern observed for the "complex phase" and for our "whitish state". At higher temperatures ($\chi_{S-P} = 0.03$, Figure 10B) with the same degree of water contamination, two ordered phases may be observed, one the lower polymer concentration ordered phase ("normal cholesteric" spacing) and the other the higher polymer concentration ordered phase (the "complex phase"?). This is consistent with Figure 4. What remains to be understood is the X-ray spacing observed for the "complex" phase. A 32-Å spacing would correspond to less than 20 vol % polymer if simple cholesteric hexagonal packing of rods were assumed (see Figure 3). However, the diffraction pattern from the "complex phase" shows several spacings. This was interpreted by Luzzati et al. to correspond to a twisted triple-helical, superhelical, or "coiled-coil structure".[11] Later, Parry and Elliott,[12] using fiber orientation and a gold-focused camera, showed convincingly that a different interpretation was correct. Their model had the polymer molecules enjoined in a very complex intermolecular stacking of side-chain benzene rings and an *incomplete hexagonal arrangement* that contains more than one polymer molecule per unit cell, as shown in Figure 11. Our less detailed diffraction pattern is quite consistent with theirs, as pointed out earlier, which makes

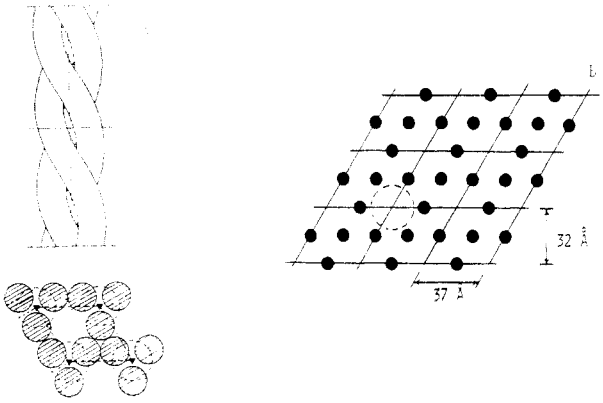

Figure 11. Proposed structure of the "complex phase" deduced from X-ray diffraction by Luzzati et al.[11] (A) or Parry and Elliott[12] (B).

us feel that our "whitish state" is the same as the "complex phase". However, the methods of sample preparation differ markedly. Our samples were homogeneously prepared by stirring at elevated temperatures. Luzzati et al. also prepared directly a polymer–diluent solution.[11] Parry and Elliott prepared their samples by adding DMF to dry fibers drawn from dioxane solutions. Our "whitish state" X-ray patterns depended only on temperature. By being taken in a random temperature sequence, equilibrium structures are indicated. No information concerning equilibrium in the DMF-dampened fibers is available.[12] Assuming the packing shown in Figure 11 is correct and assuming a PBLG density of 1.26 g cm^{-3}, the volume fraction polymer in the "whitish state" or "complex phase" would be 48% polymer. This is less than that predicted by the Flory model and also less than that found by isopiestic measurements using dry DMF.[14] However, the Flory model assumes random packing and not a specific structure as in Figure 11. The composition of the high-concentration Flory model phase boundary will depend on the details of the model and on the model chosen.[19,21] It should also be noted, on the basis of limited studies, that a dry, i.e., clear, PBLG/DMF sample (a true binary) cooled to the isotropic–liquid crystal wide biphasic region does not show the "complex phase" X-ray diffraction pattern. It could thus be that the general features of the ternary diagrams are appropriate to explain the complex phase, but the detailed structure may be a result of having the third component present. It is unknown whether or not these remarks are applicable to the "complex phase" also reported with pyridine as the solvent[11] or to the biphasic behavior reported for poly(γ-methyl D-glutamate) in pyridine.[23]

The discrepancy between the ca. 48% concentration by X-ray and the 65% or larger value found by isopiestic measurements is troubling. We feel strongly that the 32-Å infrastructure spacing is an equilibrium value. However, the degree to which vacant sites in this framework are filled may depend on sample history. For example, the vacant sites may be filled very slowly when the concentrated phase is approached by phase separation of a sample with lower bulk composition. On the other hand, we can think of no reason why a dampened fiber would form a structure with vacant sites[12] unless that structure was at lower energy for the particular solvent. Therefore, the most likely explanation for the unexpectedly low concentration of the ordered phase in whitish samples lies in the ternary phase diagram, where it may be seen that water contamination lowers the concentration in the ordered phase. Difficulty in preparing and sealing, without introducing water, very concentrated, homogeneous solutions of PBLG/DMF have prevented us from examining this point in greater detail.

The answer to the third question, the whitish appearance of the water-wet PBLG/DMF samples compared to the clear appearance in dry DMF whether in the single-phase liquid crystal region or even in the wide biphasic region, may be a result of the differences in refractive indices among the components. The refractive index of H_2O is 1.33, that of DMF is 1.43, and the refractive index increment of adding PBLG to DMF is 0.12 $cm^3\ g^{-1}$. Thus if the complex phase is a dilute isotropic polymer solution in equilibrium with a high-concentration (48 vol %) ordered phase, which may be interconnected to form a network, differential water partitioning to the isotropic phase may lead to the whitish, opaque appearance. Verification of this requires further study.

The final question, the appearance of periodicity spacing immediately (within 15 s) upon warming wet whitish samples to the clearing point, whereas dry DMF samples of similar polymer concentration warmed from biphasic to the single cholesteric phase may take hours or days for the periodicity spacings to appear, may be discussed by using Figures 9–11. Considering the "whitish state" to be a dilute isotropic phase in equilibrium with the ca. 50 vol % polymer structure shown in Figure 11, warming to give a cholesteric phase of 15–40 vol % polymer involves diluting the incomplete hexagonal array with solvent from the surrounding isotropic phase. This may be rapid. However, in dry DMF, raising the temperature from the wide biphasic region to that where a single liquid crystalline phase is stable (see Figure 6) requires diluting a much higher polymer concentration liquid crystalline phase containing no vacancies analogous to the complex phase. Thus the time scale to dilute and twist to give the periodicity spacings may be long.

Acknowledgment. This work was supported by the National Institutes of Health.

Registry No. Poly(γ-benzyl L-glutamate) (homopolymer), 25014-27-1; poly(γ-benzyl L-glutamate) (SRU), 25038-53-3; DMF, 68-12-2; H_2O, 7732-18-5.

References and Notes

(1) C. Robinson, *Trans. Faraday Soc.*, **52**, 571 (1956).
(2) C. Robinson, J. C. Ward, and R. B. Beevers, *Discuss. Faraday Soc.*, **25**, 29 (1958).
(3) C. Robinson, *Mol. Cryst.*, **1**, 467 (1966).
(4) R. W. Duke and D. B. DuPré, *Macromolecules*, **7**, 374 (1974).
(5) D. B. DuPré and R. W. Duke, *J. Chem. Phys.*, **63**, 143 (1975).
(6) N. S. Murthy, J. R. Knox, and E. T. Samulski, *J. Chem. Phys.*, **65**, 4835 (1976).
(7) R. W. Duke, D. B. DuPré, and E. T. Samulski, *J. Chem. Phys.*, **66**, 2748 (1977).
(8) J. Watanabe, K. Imai, and I. Uematsu, *Polym. Bull.*, **1**, 67 (1978).
(9) D. Patel and D. B. DuPré, *Mol. Cryst. Liq. Cryst.*, **53**, 323 (1979).
(10) H. Toriumi, S. Minakuchi, Y. Uematsu, and I. Uematsu, *Polym. J.*, **12**, 431 (1980).
(11) V. Luzzati, M. Cesari, G. Spack, F. Masson, and J. M. Vincent, *J. Mol. Biol.*, **3**, 566 (1961). Note: A translation by C. Cohen is found in "Polyamino Acids, Polypeptides and Proteins", M. Stahmann, Ed., University of Wisconsin Press, Madison, WI, 1962.
(12) D. Parry and A. Elliott, *J. Mol. Biol.*, **25**, 1 (1967).
(13) E. Wee and W. G. Miller, *J. Phys. Chem.*, **75**, 1446 (1971).
(14) W. G. Miller, J. H. Rai, and E. L. Wee, in "Liquid Crystals and Ordered Fluids", Vol. 2, J. F. Johnson and R. S. Porter, Eds., Plenum Press, New York, 1974, p 243.
(15) (a) S. Chakrabarti and W. G. Miller, *Biopolymers*, **23**, 719 (1984). (b) S. Chakrabarti, Ph.D. Thesis, University of Minnesota, 1982.
(16) W. G. Miller, C. C. Wu, E. L. Wee, G. L. Santee, J. H. Rai, and K. D. Goebel, *Pure Appl. Chem.*, **38**, 37 (1974).
(17) J. H. Rai and W. G. Miller, *J. Phys. Chem.*, **76**, 1081 (1972).

(18) K. D. Goebel and W. G. Miller, *Macromolecules*, **3**, 67 (1970).
(19) P. J. Flory, *Proc. R. Soc. London, Ser. A*, **234**, 73 (1956).
(20) P. S. Russo and W. G. Miller, *Macromolecules*, **16**, 1690 (1983).
(21) M. Warner and P. J. Flory, *J. Chem. Phys.*, **73**, 6327 (1980).
(22) A. Nakajima, T. Hayishi, and M. Ohmori, *Biopolymers*, **6**, 973 (1968).
(23) K. Ito, T. Kajiyama, and M. Takayanagi, *Polym. J.*, **12**, 305 (1980).

Aqueous Phase in a Perfluorocarboxylate Membrane

Noel G. Boyle, J. Michael D. Coey, A. Meagher, and Vincent J. McBrierty

Department of Pure and Applied Physics, Trinity College, Dublin 2, Ireland

Yoshitomo Nakano and William J. MacKnight*

Polymer Science and Engineering Department, University of Massachusetts, Amherst, Massachusetts 01003. *Received July 12, 1983*

ABSTRACT: A perfluorocarboxylate membrane has been characterized by dynamic mechanical relaxation, NMR on ^1H and ^{19}F, and ^{57}Fe Mössbauer spectroscopy of the ferric salt. Results are similar to those reported for perfluorosulfonate membranes, indicating that the specific charged end group has little influence on the structure or behavior of the aqueous phase. Exchanged ions in the membranes at ambient humidity and above are not directly coordinated by sulfonate or carboxylate groups, but by water. Precipitation of ferric hydroxide in a ferric membrane reexchanged with KCl is inferred from the Mössbauer spectrum at 4.2 K and confirmed by NMR relaxation times.

Introduction

The properties of perfluorosulfonate ion-exchange membranes depend sensitively upon the cation present and on the amount of absorbed water.[1-3] The behavior of the aqueous phase, in particular the glasslike character at low temperatures, has been studied in a number of membranes, but especially in Nafion[4] using techniques[1-3] which include nuclear magnetic resonance (NMR)[5-8] and Mössbauer spectroscopy.[9-11] This paper focuses upon a relative newcomer to the field, a perfluorocarboxylate membrane in which the side group is terminated with COOH rather than SO_3H. It is of interest to ascertain, for example, the relative tendency of the ionic phase to cluster, to explore the stability of the membrane with increasing temperature, and, more generally, to determine the extent to which the macroscopic properties are altered by the presence of carboxylate. NMR, Mössbauer, and mechanical relaxation results are presented and compared with data for other perfluorinated membranes. This combination of experimental probes gives microscopic information on the motions of the polymer chains, and of the ions and water which constitute the aqueous phase, besides providing a macroscopic overview of the relaxation processes.

Experimental Methods

The sample under investigation was obtained from the Asahi Glass Co. in the form of a pressed sheet 250 μm thick. The water content at ambient humidity was determined, by heating under vacuum at 423 K, to be 6 wt %. Prompted by the findings of an earlier study on Nafion[6] (as received) in which impurity iron and potassium were detected in significant amounts, we carried out an X-ray fluorescence microprobe analysis of the carboxylate sample. The results, presented in Table I, reflect similar amounts of iron and potassium impurity and indicate further a sulfur content about 60% of that recorded for a comparable volume of the acid perfluorosulfonate membrane. Additionally, a microprobe line scan showed that the sulfur was concentrated toward the membrane surfaces. If the sulfur is a constituent of SO_3H (or SO_3K) end groups, this would imply that the membrane was only about 40–45% carboxylate exchanged.

^1H and ^{19}F T_1, T_2, and $T_{1\rho}$ NMR data were recorded over the temperature range 120–380 K using the experimental procedures and methods of data analysis described previously.[8] Mössbauer spectroscopy, also described previously,[9] was applied to the Fe^{3+}-exchanged carboxylate sample. Iron was initially incorporated by stirring the membrane in a 0.2 M aqueous solution of $FeCl_3$ for 12 h and subsequently precipitated by reexchange in a solution of 0.1 M KCl. In both cases a microprobe line scan was reasonably flat across the thickness of the membrane, implying a correspondingly uniform distribution of iron across the profile. Dynamic mechanical relaxation studies were carried out with a dynamic mechanical thermal analyzer (Polymer Laboratories), operating at 1 Hz over the temperature range 180–520 K.

Membranes were conditioned by boiling in water and drying under various conditions.

Table I
Number of Iron Atoms/cm³ and Ratio of Potassium to Sulfur Content for the COOH Membrane As Received and an Acid Nafion of Comparable Water Content

sample	no. of Fe^{3+}/cm^3	K/S
COOH membrane	3.7×10^{18}	0.33
Nafion (115)	7.2×10^{18}	0.41

Results and Discussion

NMR. It is recalled that the ^1H data reflect predominantly the response of absorbed water in the membrane while the ^{19}F resonance probes the onset of molecular motion in the fluorocarbon backbone matrix. The ^1H results of Figure 1 confirm that the behavior of the aqueous phase in the perfluorocarboxylate acid membrane is in most respects comparable with that observed in a perfluorosulfonate acid Nafion of similar water content for which a detailed interpretation of NMR data, including a treatment of the role of impurity iron, was presented in two earlier papers.[5,6] Briefly, (i) the onset of general motions in the aqueous phase, typical of a glass transformation process (T_g = 182 K), was evident in the sharp rise in T_2 near 170 K and in the formation of $T_{1\rho}$ and T_1 minima at ~180 and ~230 K, respectively; (ii) as temperature increased, chemical exchange between heterogeneous water sites was presumed to set in and to become fully activated near ambient temperature; (iii) comparison of the magnitudes of the NMR relaxation times as a function of iron content implied that the iron in the membrane as received was most probably in the aqueous phase and that $T_{1\rho}$ was much less sensitive than T_1 or T_2 to the presence of iron. Either $T_{1\rho}$ is dominated by mo-

0024-9297/84/2217-1331$01.50/0